IOP Concise Physics

Topological Insulators

Panagiotis Kotetes

Chapter 1

Symmetries and effective Hamiltonians

In this chapter we introduce a number of symmetry concepts that play a key role in predicting and analysing topological phenomena. First we provide an introduction to unitary and antiunitary symmetry transformations and afterwards unfold a programme of how to employ them for retrieving symmetry-invariant effective Hamiltonians. We specifically focus on models for III–V semiconductors, which are particularly relevant for the topological systems to be studied later. One should note that the invariance of a system under a set of symmetries not only serves as an indispensable tool for performing technical analysis, but is essentially decisive for the arising topological properties.

1.1 Crash course on symmetry transformations

By and large, the behaviour of material systems and other abstract objects under the action of a group of symmetry transformations, allows us to categorise them into distinct classes. The members of a given class share common features and characteristics tied to the ensuing symmetry. An abstract object is said to exhibit a particular symmetry when it remains invariant under the corresponding symmetry transformation or operation, cf textbooks such as [1–5]. For example, an ideal planar disc is symmetric or invariant under arbitrary rotations about its out-of-plane axis. This, in turn, implies that the coordinate vector of a given point on the disc transforms in a specific fashion under rotations. Apart from spatial rotations, symmetry tranformations additionally include operations such as reflections, inversion and translations, while the last two are also extended to the time dimension. More importantly, one can also define symmetries not associated with the physical spacetime but rather with a type of internal or parameter space related, for instance, to isospin, flavour, colour, valley or other degrees of freedom.

When symmetry transformations are defined in the Hilbert space of a given quantum-mechanical system, they are usually considered to yield an O-symmetry when the respective operator effecting the symmetry $\hat{O}$, leaves the Hamiltonian ($\hat{H}$)

doi:10.1088/978-1-68174-517-6ch1

invariant, i.e. $\hat{O}^{\dagger}\hat{H}\hat{O} = \hat{H} \Rightarrow [\hat{O}, \hat{H}] = \hat{0}$ [1]. As a result, the presence of symmetry leads to energy degeneracies for two (or more) Hamiltonian eigenstates with quantum numbers $a \neq b$, i.e. $E_a = E_b$. While this corresponds to the conventional and most often used definition, one can extend the notion of symmetry to include also those which instead yield a sign change of the Hamiltonian, i.e. $\hat{O}^{\dagger}\hat{H}\hat{O} = -\hat{H} \Rightarrow \{\hat{O}, \hat{H}\} = \hat{0}$ [6–8]. Symmetries of this kind are crucial for predicting and describing the topological properties of a system. This will become clear in the upcoming chapters and especially in chapter 8. While these symmetries do not generally imply degeneracies, they still impose constraints on the energy spectrum, e.g. $E_a = -E_b$. Finally, the operators effecting symmetry transformations can be split into two categories, the unitary (O_u) and antiunitary (O_a), which can be distinguished by their different action on a complex c-number z, i.e. $\hat{O}_u^{\dagger} z \hat{O}_u = z\hat{1}$ and $\hat{O}_a^{\dagger} z \hat{O}_a = z^{*}\hat{1}$, with $\hat{1}$ the identity operator.

1.1.1 Unitary symmetry transformations

Here we introduce the unitary symmetries by considering the case of a spinless particle described by a wavefunction ϕ, that is a solution of the time-independent single-particle Schrödinger equation $\hat{H}\phi = E\phi$ [1], with E denoting the particle's energy. Within the quantum-mechanical description, a symmetry transformation acts on a wavefunction which depends on the particle's coordinate $\boldsymbol{r}$ in the following manner

$$\phi' \coloneqq O\phi \quad \text{and} \quad \phi'(\boldsymbol{r}) = \hat{O}\phi(\boldsymbol{r}), \tag{1.1}$$

where $\hat{O}$ corresponds to the symmetry-transformation operator, defined in the given $\boldsymbol{r}$ basis. For instance, if we wish to translate the system by a along the direction defined by the unit vector $\check{\boldsymbol{n}}$, i.e. $\boldsymbol{r}' = \boldsymbol{r} + a\check{\boldsymbol{n}}$, we must act on $\phi(\boldsymbol{r})$ with the translation operator $\hat{t}_a^{\check{\boldsymbol{n}}} = e^{-\mathrm{i}a\check{\boldsymbol{n}}\cdot\hat{\boldsymbol{p}}/\hbar}$ [1], where $\hat{\boldsymbol{p}}$ defines the momentum operator which, in the position basis, is represented as $\hat{\boldsymbol{p}} = \hbar\nabla/\mathrm{i}$. It is straightforward to see that for an infinitesimal translation a along $\check{\boldsymbol{n}}$, we have

$$\begin{aligned}\phi'(\boldsymbol{r}) &= e^{-\mathrm{i}a\check{\boldsymbol{n}}\cdot\hat{\boldsymbol{p}}/\hbar}\phi(\boldsymbol{r}) \approx (1 - \mathrm{i}a\check{\boldsymbol{n}}\cdot\hat{\boldsymbol{p}}/\hbar)\phi(\boldsymbol{r}) \\ &= (1 - a\check{\boldsymbol{n}}\cdot\nabla)\phi(\boldsymbol{r}) \approx \phi(\boldsymbol{r} - a\check{\boldsymbol{n}}) \equiv \phi\left(t_a^{-\check{\boldsymbol{n}}}\boldsymbol{r}\right).\end{aligned} \tag{1.2}$$

Note that, in the above, the transformation acts in the argument in the inverse sense compared to the wavefunction. Such a transformation property was anticipated, since the existence of a symmetry transformation implies that we can equivalently write for the scalar wavefunction

$$\phi'(\boldsymbol{r}') = \phi(\boldsymbol{r}) \quad \Rightarrow \quad \phi'(\boldsymbol{r}) = \phi(\boldsymbol{r} - a\check{\boldsymbol{n}}). \tag{1.3}$$

In a similar fashion, a rotation by an angle θ about an axis with direction $\check{\boldsymbol{n}}$ would be effected using the rotation operator $\hat{R}_{\theta}^{\check{\boldsymbol{n}}} = e^{-\mathrm{i}\theta\check{\boldsymbol{n}}\cdot\hat{\boldsymbol{L}}/\hbar}$ [1], where $\hat{\boldsymbol{L}} = \hat{\boldsymbol{r}} \times \hat{\boldsymbol{p}}$ defines the orbital angular momentum operator. If the wavefunction $\phi(\boldsymbol{r})$ is instead a spinor $\boldsymbol{\phi}(\boldsymbol{r})$, then a rotation will be generated by the total angular momentum $\hat{\boldsymbol{J}} = \hat{\boldsymbol{L}} + \hat{\boldsymbol{S}}$, with $\hat{\boldsymbol{S}}$ denoting the spin angular momentum operator. A spinor corresponding to

spin s, has $2s + 1$ components labelled by the quantum number $m_s = s, s - 1, \ldots, -s$:

$$\boldsymbol{\phi}(\boldsymbol{r}) = \left(\phi_s(\boldsymbol{r}), \phi_{s-1}(\boldsymbol{r}), \ldots, \phi_{-s}(\boldsymbol{r})\right)^{\mathrm{T}}, \tag{1.4}$$

with T denoting matrix transposition. For a spin-1/2 particle, $m_s = \pm\frac{1}{2}$, and we have

$$\boldsymbol{\phi}(\boldsymbol{r}) = \left(\phi_{+\frac{1}{2}}(\boldsymbol{r}), \phi_{-\frac{1}{2}}(\boldsymbol{r})\right)^{\mathrm{T}} \coloneqq \left(\phi_{\uparrow}(\boldsymbol{r}), \phi_{\downarrow}(\boldsymbol{r})\right)^{\mathrm{T}} \tag{1.5}$$

and the spin operator assumes the form $\hat{\boldsymbol{S}} = \hbar\hat{\boldsymbol{\sigma}}/2$, where $\hat{\boldsymbol{\sigma}}$ define the Pauli matrices [1]

$$\hat{\sigma}_x = \begin{pmatrix} 0 & 1 \\ 1 & 0 \end{pmatrix}, \quad \hat{\sigma}_y = \begin{pmatrix} 0 & -\mathrm{i} \\ \mathrm{i} & 0 \end{pmatrix} \quad \text{and} \quad \hat{\sigma}_z = \begin{pmatrix} 1 & 0 \\ 0 & -1 \end{pmatrix}. \tag{1.6}$$

The corresponding rotation operator $e^{-\mathrm{i}\theta\check{\boldsymbol{n}}\cdot\hat{\boldsymbol{S}}/\hbar}$, reads

$$e^{-\mathrm{i}\theta\check{\boldsymbol{n}}\cdot\hat{\boldsymbol{\sigma}}/2} = \cos(\theta/2)\hat{1}_{\sigma} - \mathrm{i}\sin(\theta/2)\check{\boldsymbol{n}}\cdot\hat{\boldsymbol{\sigma}}, \tag{1.7}$$

with $\hat{1}_{\sigma}$ denoting the identity matrix in spin space. The factor of 1/2 implies that the above operator exhibits a 4π, instead of 2π, periodicity with respect to θ. Contrary to the wavefuctions and spin rotation operator, the spin operators $\hat{\boldsymbol{S}}$ are connected to physical observables and thus exhibit a 2π periodicity, as shown in section 1.1.2. For more details see section 1.2.2.

In addition to the above continuous symmetry transformations, one can also introduce discrete ones, such as spatial inversion and reflections. In three spatial dimensions ($d = 3$), inversion (I) has the following action: $I\{\boldsymbol{r}, \boldsymbol{p}, \boldsymbol{L}\} = \{-\boldsymbol{r}, -\boldsymbol{p}, \boldsymbol{L}\}$. The angular momentum does not change sign, since it constitutes a pseudovector. Remarkably, the situation changes for a strictly two-dimensional system, where I can flip the sign of the angular momentum components. The reason is that in $d = 2$, I describes a transformation which is equivalent to a proper rotation, similar to that generated by $\hat{\boldsymbol{J}}$. This should be contrasted with $d = 3$, in which I effects an improper rotation. The distinction between proper and improper rotations relies on the sign of the determinant of the rotation matrix, being positive and negative, in each case respectively. As a matter of fact, for systems defined in odd spatial dimensions, inversion also effects parity. The latter is defined as a discrete improper rotation in all dimensions. For a system confined in the xy plane, the two-dimensional version of parity coincides with reflections σ_v, with 'v' denoting the presence of a vertical mirror symmetry plane. For example, the reflection or mirror operation σ_{xz}, effects the transformation $(x, y) \mapsto (x, -y)$. In general, an improper rotation defined in even spatial dimensions is equivalent to the combination of a proper rotation and an inversion, when the system is embedded in a space with one extra spatial dimension. For an example see Hands-on section 1.3.

1.1.2 Action of symmetry transformations on operators

Having retrieved the transformation properties of the wavefunctions under a symmetry operation, we can readily determine the transformation of any operator,

$\hat{A}$, associated with a physical observable. This is achieved by requiring that the matrix elements of the operator remain unchanged. We define:

$$\int d\boldsymbol{r}\ \phi^*(\boldsymbol{r})\hat{A}'\psi(\boldsymbol{r}) \coloneqq \int d\boldsymbol{r}\ [\phi'(\boldsymbol{r})]^*\hat{A}\psi'(\boldsymbol{r}) = \int d\boldsymbol{r}\ \phi^*(\boldsymbol{r})\hat{O}^\dagger\hat{A}\hat{O}\psi(\boldsymbol{r}), \tag{1.8}$$

for arbitrary $\phi(\boldsymbol{r})$ and $\psi(\boldsymbol{r})$ which implies

$$\hat{A}' \coloneqq O\hat{A} \equiv \hat{O}^\dagger\hat{A}\hat{O}. \tag{1.9}$$

Interestingly, for the particular description of our coordinate-space-defined wavefunctions, we can also view the position vector $\boldsymbol{r}$, as an operator $\hat{\boldsymbol{r}}$. Therefore, equation (1.9) allows us to verify that for a translation $\hat{t}_a^{\check{\boldsymbol{n}}}$, one obtains

$$\hat{\boldsymbol{r}}' = \left(\hat{t}_a^{\check{\boldsymbol{n}}}\right)^\dagger\hat{\boldsymbol{r}}\hat{t}_a^{\check{\boldsymbol{n}}} = e^{\mathrm{i}a\check{\boldsymbol{n}}\cdot\hat{\boldsymbol{p}}/\hbar}\hat{\boldsymbol{r}}\ e^{-\mathrm{i}a\check{\boldsymbol{n}}\cdot\hat{\boldsymbol{p}}/\hbar} = \hat{\boldsymbol{r}} + a\check{\boldsymbol{n}}. \tag{1.10}$$

This result was expected, as according to the definition of $\hat{A}'$ given in equation 1.8, we essentially consider that we transform the Hamiltonian system rather than the coordinate system, i.e. we employ the so-called active view of symmetry transformations [1, 3]. We could alternatively employ the passive point of view of symmetry transformations via the definition $\int d\boldsymbol{r}\ \phi^*(\boldsymbol{r})\hat{A}\psi(\boldsymbol{r}) \coloneqq \int d\boldsymbol{r}\ [\phi'(\boldsymbol{r})]^*\hat{A}'\psi'(\boldsymbol{r})$ that instead yields $\hat{A}' = \hat{O}\hat{A}\hat{O}^\dagger$. Throughout this book we always employ the *active* view. Furthermore, note that for more general operators, which are not defined in a Hilbert space, we have $\hat{A}' = \hat{O}^{-1}\hat{A}\hat{O}$ [3, 5].

As an example, we investigate the transformation of the spin operators $(\hat{S}_x, \hat{S}_y)$, under a rotation by an angle θ about the z axis. For simplicity, we consider the case of a spin-1/2 particle, where we can equivalently study the transformation of the $\hat{\sigma}_{x,y}$ Pauli matrices. Equation (1.9) yields:

$$R_\theta^{\hat{z}}\begin{pmatrix}\hat{\sigma}_x\\ \hat{\sigma}_y\end{pmatrix} = e^{\mathrm{i}\theta\hat{z}\cdot\hat{\boldsymbol{\sigma}}/2}\begin{pmatrix}\hat{\sigma}_x\\ \hat{\sigma}_y\end{pmatrix}e^{-\mathrm{i}\theta\hat{z}\cdot\hat{\boldsymbol{\sigma}}/2} = \begin{pmatrix}\cos\theta & -\sin\theta\\ \sin\theta & \cos\theta\end{pmatrix}\begin{pmatrix}\hat{\sigma}_x\\ \hat{\sigma}_y\end{pmatrix}. \tag{1.11}$$

From this we observe that the spin operator $\hat{\boldsymbol{S}}$, exhibits a 2π periodicity under spatial rotations and transforms in a similar way to $\hat{\boldsymbol{r}}$.

1.1.3 Antiunitary symmetry transformations: time reversal

The most familiar example of an antiunitary symmetry transformation is time reversal (TR) $\mathcal{T}$, effected by taking $t \to -t$. The time-reversed partner of a spinless particle's wavefunction $\phi(\boldsymbol{r}, t)$, is $\mathcal{T}\phi(\boldsymbol{r}, t) = \phi^*(\boldsymbol{r}, -t)$. The time-reversed Hamiltonian simply reads $\mathcal{T}\hat{H}(t) = \hat{H}^*(-t)$, since we are dealing with an antiunitary symmetry transformation operator. The explicit action of complex conjugation can be replaced by introducing the respective operation K, thus $\mathcal{T}\hat{H}(t) = K\hat{H}(-t)$. Note that $\hat{K}^2 = \hat{1}$ and its action on the position, momentum and orbital angular momentum operators is [1]

$$K\hat{\boldsymbol{r}} = \hat{\boldsymbol{r}}, \qquad K\hat{\boldsymbol{p}} = -\hat{\boldsymbol{p}} \qquad \text{and} \qquad K\hat{\boldsymbol{L}} = -\hat{\boldsymbol{L}}. \tag{1.12}$$

From this we conclude that for spinless particles governed by time-independent Hamiltonians, $\mathcal{T} \equiv K$. Consequently, $\mathcal{T}$-symmetric time-independent Hamiltonians for spinless particles are necessarily real, while the action of $\mathcal{T}$ on the above operators also reads

$$\mathcal{T}\hat{\boldsymbol{r}} = \hat{\boldsymbol{r}}, \qquad \mathcal{T}\hat{\boldsymbol{p}} = -\hat{\boldsymbol{p}} \qquad \text{and} \qquad \mathcal{T}\hat{\boldsymbol{L}} = -\hat{\boldsymbol{L}}. \tag{1.13}$$

In the case of spinful particles we have to retrieve the action of $\mathcal{T}$ on the spin operator $\hat{\boldsymbol{S}}$. Since the latter represents a type of angular momentum, it transforms in the same manner as $\hat{\boldsymbol{L}}$. Thus $\mathcal{T}\hat{\boldsymbol{S}} = -\hat{\boldsymbol{S}}$. Given the freedom to choose a representation in which $\hat{S}_{x,z}$ are real and $\hat{S}_y$ imaginary (see [1]), we can employ K and rewrite the $\hat{\mathcal{T}}$ operator as

$$\hat{\mathcal{T}} = e^{i\pi\hat{S}_y/\hbar}\hat{K}. \tag{1.14}$$

Given this representation, $\mathcal{T}$ is generated by the successive operations of K and a π rotation in spin space about the y axis, since $K(\hat{S}_x, \hat{S}_y, \hat{S}_z) = (\hat{S}_x, -\hat{S}_y, \hat{S}_z)$.

For spin-1/2 fermions (e.g. electrons) we have $\hat{S}_y = \hbar\hat{\sigma}_y/2$, which implies $\hat{\mathcal{T}} = i\hat{\sigma}_y\hat{K}$ and $\mathcal{T}\hat{H} = \hat{\sigma}_y\hat{K}^\dagger\hat{H}\hat{K}\hat{\sigma}_y$. Notice that $\hat{\mathcal{T}}^2 = -\hat{1}$, which is a characteristic of systems with half-integer spin. In contrast, for systems with integer spin, we obtain $\hat{\mathcal{T}}^2 = \hat{1}$. In the first case, the negative sign yields the celebrated Kramers degeneracy, i.e. every Hamiltonian eigenenergy is doubly degenerate and the two eigenstates are connected by TR. As an example consider the case of electrons in the absence of a magnetic field, in which the spin-up and -down states are degenerate. However, if $\hat{\mathcal{T}}^2 = \hat{1}$, $\mathcal{T}$ behaves in a similar way to K. In this case, the presence of time-reversal symmetry (TRS), with an operator squaring to identity, imposes a reality constraint on the Hamiltonian; i.e. by an appropriate choice of basis, the Hamiltonian can be represented as a real matrix and characterised by real eigenvectors [1].

1.1.4 Symmetry groups

In the previous paragraphs we provided some examples of symmetry transformations. However, a real material or abstract system can be simultaneously invariant under a set of symmetries. One finds that the various symmetry transformations may be interrelated, thus construing symmetry groups. A collection of elements A, B, C, … form a group $\mathcal{G}$, when the following conditions are met [4]:

1. The product of any two group elements yields another group element, i.e. $AB = C$, with $A, B, C \in \mathcal{G}$.
2. The elements satisfy the associative law: $(AB)C = A(BC)$.
3. There exists an identity element, E, commuting with any other group element A, i.e. $EA = AE$.
4. Every element has an inverse: $AA^{-1} = A^{-1}A = E$.

In order to make the term symmetry group more transparent, let us give the following example. Assume the time-independent Schrödinger equation $\hat{H}\phi = E\phi$

for a localised spin-1/2 particle in a magnetic field oriented along the z spin axis, for which, the Zeeman coupling yields $\hat{H} = -E_{\text{Zeeman}}\hat{\sigma}_z$. Due to the properties of the Pauli matrix, $\hat{\sigma}_z^2 = \hat{1}$, and one finds that $\hat{H}^2 = E_{\text{Zeeman}}^2\hat{1}$. Thus, the eigenvalues of the Hamiltonian are given by $E_\pm = \pm E_{\text{Zeeman}}$, implying that the respective eigenstates $|\phi_\pm\rangle$ satisfy $\hat{H}|\phi_\pm\rangle = \pm E_{\text{Zeeman}}|\phi_\pm\rangle$. Note that every Hamiltonian squaring to a constant will have the same eigenvalue structure and will lead to a similar relation for its eigenvectors. The details of the physical system under consideration solely fix the energy scale and the exact expression of the eigenvectors. These statements can be also extended to operators effecting symmetry transformations. For example, inversion satisfies $\hat{I}^2 = \hat{1}$ and thus it is characterised by the same general type of eigenvalues and eigenvectors as the Hamiltonian above.

Instead of eigenvalues and eigenvectors, a more appropriate nomenclature applying for symmetry transformations is characters and irreducible representations. In fact, the characters and irreducible representations characterise a symmetry group and not a single symmetry transformation. Notably, a group structure has made its appearance already in the discussion above. For the case of inversion, I and I^2 form a group. I^2 constitutes the identity element of the group, commmonly denoted with E. Since the two symmetry tranformations commute, i.e. $EI = IE$, the group is *Abelian*. In general, a symmetry group consists of a finite or an infinite number of elements, which defines the *order* of the group, h_G. The elements of a group do not necessarily commute and the group is in this case called *non-Abelian*.

For the group $\{E, I\}$ there exist two irreducible representations A_1 and A_2, coinciding with the representations of the group elements when acting on $|\phi_+\rangle$ and $|\phi_-\rangle$, respectively. In the A_1 irreducible representation: $\{E, I\} = \{1, 1\}$, while in the A_2: $\{E, I\} = \{1, -1\}$. Note that these irreducible representations are one-dimensional, since the $|\phi_\pm\rangle$ transform into themselves under the action of the symmetry-group elements. However, non-Abelian groups support multi-dimensional irreducible representations, in which, each symmetry group element is represented by a matrix. The trace of the representation matrix defines the so-called character $\chi_{\text{IR}}(g)$ of the symmetry group element g, in the given irreducible representation IR. For one-dimensional irreducible representations the character coincides with the representation itself. Consequently, here we find $\chi_{A_1} = \{1, 1\}$ and $\chi_{A_2} = \{1, -1\}$.

While the scope of this work is not an in-depth group theory study (for more details refer to [1–5]), we present in the following section an example of how to analyse the C_{3v} symmetry point group, arising for instance in a triangularly-arranged triple-quantum-dot device.

C_{3v} point-group symmetry example: triangular triple-quantum-dot device

In the following paragraphs we provide an example regarding symmetry groups and, in particular, how to derive their irreducible representations. The model system for this purpose is a lateral triple-quantum-dot (TQD) device where the three dots are assumed identical and arranged in a triangular fashion [9, 10] as in

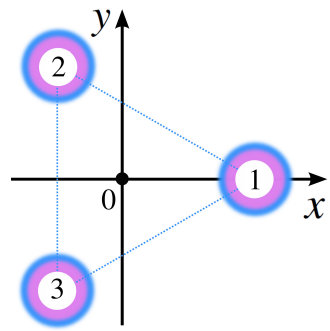

Figure 1.1. Three identical quantum dots arranged in a triangular fashion. The emergent triangle is equilateral, thus leading to a C_{3v} point group symmetry. This point-group consists of the identity element E, the C_3 counterclockwise rotation ($\{1, 2, 3\}\mapsto\{2, 3, 1\}$), the $C_3^2 \equiv C_3^{-1}$ clockwise rotation ($\{1, 2, 3\}\mapsto\{3, 1, 2\}$), the σ_{xz} mirror operation ($\{1, 2, 3\}\mapsto\{1, 3, 2\}$), the $C_3\sigma_{xz}$ mirror operation ($\{1, 2, 3\}\mapsto\{3, 2, 1\}$) and the $C_3^2\sigma_{xz}$ mirror operation ($\{1, 2, 3\}\mapsto\{2, 1, 3\}$).

figure 1.1. In the Hands-on section 1.3, we additionally demonstrate how to obtain effective Hamiltonians for the TQD system using group theoretical approaches.

Quantum dots constitute 'zero'-dimensional, electrostatically-confined (see section 1.2.4) or self-assembled, islands of electrons in which the finite-size effects lead to a discrete-only energy spectrum, since their diameter is of the order of a few to a few-hundred nanometers. Due to the complete confinement-induced energy level quantisation, they have been termed as *artificial atoms* [11]. Notably, while the number of electrons in a quantum dot can be large, the energy for adding an extra electron relative to a reference number can be finely tuned via electrostatic gating, thus allowing one to controllably create a few-excess-electron subsystem on the dot.

In the following, we consider a TQD with a single excess electron relative to the reference. Thus, a single-particle Hamiltonian is sufficient for examining the properties of the system. Nonetheless, even without specifying any further details for the TQD, we can already phenomenologically write down the most general Hamiltonian that may describe this system, solely based on the notion of its symmetries. We unfold the programme for reaching this goal below and in Hands-on section 1.3.

The three identical dots are deposited on a substrate and assumed to be perfectly aligned so to give rise to an equilateral triangle. The given structure is characterised by invariance under a set of $2\pi/3$ rotations about the out-of-plane z axis. A counterclockwise rotation of the TQD is termed a C_3 rotation, with the order n, of a rotation $2\pi/n$, being $n = 3$. One also finds the inverse rotation C_3^{-1} which rotates the TQD in a clockwise fashion. Furthermore, one finds $C_3^3 = E$ and $C_3^2 = C_3^{-1}$. Thus, the set $\{E, C_3, C_3^2\}$ forms a symmetry group, termed C_3. Nevertheless, the TQD is also dictated by the set $\{\sigma_{xz}, C_3\sigma_{xz}, C_3^2\sigma_{xz}\}$ of mirror symmetries.

These symmetry transformations exhaust all the possible unitary operations that leave the TQD invariant and form the so-called C_{3v} group. Note that C_3 is a subgroup of C_{3v}. Both groups constitute *point groups*, since they consist of elements that, when they act on the system, keep at least one point fixed. After having

identified the symmetry-group elements we have to: (i) construct the multiplication table, (ii) retrieve the conjugacy classes, and (iii) obtain the irreducible representations that provides the character table. Below we appose a step-by-step presentation of this programme; for more details see [2–5].

1. *Multiplication table.* The particular table consists of all the products of two elements of the group and it also reflects its Abelian or non-Abelian structure. In the particular example we obtain table 1.1.
2. *Conjugacy classes.* The conjugacy classes divide the symmetry-group elements into sets of transformations with common features and the same character χ. For the given example one expects to find three classes. The first solely consists of the identity element $\{E\}$ and is present in every group. The second is built by the two rotations $\{C_3,\ C_3^2\}$, and the last is spanned by the mirror operations $\{\sigma_{xz},\ C_3\sigma_{xz},\ C_3^2\sigma_{xz}\}$. Mathematically, two group elements $g_{1,2}$ are conjugate if they satisfy $g_1 = g_3 g_2 g_3^{-1}$, where g_3 is an arbitrary element of the group [4]. Based on this definition, we indeed recover the three conjugacy classes mentioned above. Identifying the conjugacy classes is of utter importance, since the number of conjugacy classes coincides with the number of irreducible representations.
3. *Irreducible representations and character table.* After having identified the conjugacy classes of the symmetry group we can proceed with identifying the irreducible representations. This is greatly facilitated by the fact that the number of irreducible representations equals the number of conjugacy classes and if l_j denotes the dimensionality of the jth irreducible representation, then $\sum_j l_j^2 = h_{\mathcal{G}}$. In our case the order of the symmetry group is $h_{\mathcal{G}} = 6$, and we have three irreducible representations, therefore $l_1^2 + l_2^2 + l_3^2 = 6$. One of these irreducible representations is the identity one (A_1), which is one-dimensional. In the A_1 representation all the elements are equal to one, by definition. The above relation yields the additional one-dimensional (A_2) and two-dimensional (E) irreducible representations. Note that the characters of the irreducible representations satisfy the orthogonality condition [2–5]

$$\sum_g \chi^*_{\mathrm{IR}_i}(g)\chi_{\mathrm{IR}_j}(g) = h_{\mathcal{G}}\delta_{i,j}, \tag{1.15}$$

Table 1.1. Multiplication table of the C_{3v} point group.

·	E	C_3^2	C_3	σ_{xz}	$C_3\sigma_{xz}$	$C_3^2\sigma_{xz}$
E	E	C_3^2	C_3	σ_{xz}	$C_3\sigma_{xz}$	$C_3^2\sigma_{xz}$
C_3	C_3	E	C_3^2	$C_3\sigma_{xz}$	$C_3^2\sigma_{xz}$	σ_{xz}
C_3^2	C_3^2	C_3	E	$C_3^2\sigma_{xz}$	σ_{xz}	$C_3\sigma_{xz}$
σ_{xz}	σ_{xz}	$C_3\sigma_{xz}$	$C_3^2\sigma_{xz}$	E	C_3^2	C_3
$C_3\sigma_{xz}$	$C_3\sigma_{xz}$	$C_3^2\sigma_{xz}$	σ_{xz}	C_3	E	C_3^2
$C_3^2\sigma_{xz}$	$C_3^2\sigma_{xz}$	σ_{xz}	$C_3\sigma_{xz}$	C_3^2	C_3	E

with χ the respective characters. The sum is over all the elements $g \in \mathcal{G}$. The above orthogonality condition can directly provide the A_2 one-dimensional irreducible representation. The orthogonality of $A_{1,2}$ yields the character relation: $1 + 2\chi_{A_2}(C_3) + 3\chi_{A_2}(\sigma_{xz}) = 0$. The latter immediately provides the A_2 irreducible representation in which $\chi_{A_2}(E) = 1$, $\chi_{A_2}(C_3) = 1$ and $\chi_{A_2}(\sigma_{xz}) = -1$. To identify the two-dimensional irreducible representation, we do not need to further stick to the particular TQD system, since the former constitutes a property of the group and not of the particular physical system under consideration. Thus, we can alternatively consider any two abstract objects, of our convenience, that transform into each other under the action of C_{3v} according to the two-dimensional irreducible representation. For example, we can simply study how the above rotations and mirror symmetries act on the position vector in two dimensions (x, y). The result in this case is easy to find, since a counterclockwise rotation of angle θ about the z axis reads

$$R_\theta^z \begin{pmatrix} x \\ y \end{pmatrix} = \begin{pmatrix} \cos\theta & -\sin\theta \\ \sin\theta & \cos\theta \end{pmatrix} \begin{pmatrix} x \\ y \end{pmatrix}. \tag{1.16}$$

We therefore find the two matrices

$$\hat{C}_3 = \begin{pmatrix} -1/2 & -\sqrt{3}/2 \\ \sqrt{3}/2 & -1/2 \end{pmatrix} \quad \text{and} \quad \hat{\sigma}_{xz} = \begin{pmatrix} 1 & 0 \\ 0 & -1 \end{pmatrix}. \tag{1.17}$$

The above matrix representations of the operators generating C_3 and σ_{xz} yield $\chi_E(E) = 2$, $\chi_E(C_3) = -1$ and $\chi_E(\sigma_{xz}) = 0$. Note, however, that we have not yet verified if the above representation is indeed irreducible. In fact, instead it can be a *reducible* one, decomposable according to one of the following patterns: (i) $A_1 + A_1$, (ii) $A_2 + A_2$, or (iii) $A_1 + A_2$. To exclude this possibility we verify via equation (1.15) that the given representation is indeed orthogonal to A_1 and A_2 and thus inequivalent to both. In tables 1.2 and 1.5 we present the character table for C_{3v}.

1.1.5 Translations, Bloch's theorem and space groups

A large part of this book focuses on crystalline systems which, apart from point-group symmetries, additionally exhibit invariance under translations. The combination of the latter two kinds of symmetries yields the so-called space groups. In $d = 2$ there exist 17 space groups, also called wallpaper groups. However, in $d = 3$ we find 230 space

Table 1.2. Character table of the C_{3v} point group.

Irr. Rep.	E	$2C_3$	$3\sigma_v$
A_1	1	1	1
A_2	1	1	−1
E	2	−1	0

groups, see [4]. While studying space groups is not on the agenda of this work, we will examine some properties of translations and introduce Bloch's theorem [12].

Translations, represented here as $t_a^{\check{n}}$, constitute an Abelian group since two translation operations commute. Assume a finite-sized three-dimensional crystal with dimensions $L_x = N_x a$, $L_y = N_y b$ and $L_z = N_z c$, where a, b, c denote the lattice constants and $N_{x,y,z}$ the respective number of unit cells along the $\check{\boldsymbol{x}}$, $\check{\boldsymbol{y}}$ and $\check{\boldsymbol{z}}$ directions. By employing periodic boundary conditions one finds that $(t_a^{\check{x}})^{N_x} = E$. Similar conditions hold for the other two operations. The particular constraint on the translation operations yields their one-dimensional irreducible representations, which coincide with the respective characters. For $t_a^{\check{x}}$, the irreducible representations are essentially retrieved using the roots of $t^{N_x} = 1 \Rightarrow t_n = e^{\mathrm{i}2\pi n/N_x}$ with $n = 0, 1, 2, \ldots, N_x - 1$. For convenience, one introduces the wavenumber $k_x \coloneqq 2\pi n/L_x$ $(n = 0, 1, 2, \ldots, N_x - 1)$ and thus the irreducible representations become $t_{k_x} = e^{\mathrm{i}k_x a}$. When $L_x \to \infty$ we may treat k_x as a continuous variable. A similar procedure for the remaining two operators allows us to introduce the wavevector (or quasimomentum) $\boldsymbol{k} \coloneqq 2\pi(\frac{n}{L_x}, \frac{m}{L_y}, \frac{l}{L_z})$ with $n = 0, 1, 2, \ldots, N_x - 1$, $m = 0, 1, 2, \ldots, N_y - 1$ and $l = 0, 1, 2, \ldots, N_z - 1$.

With the above set of wavevectors we can introduce the so-called 1st Brillouin zone (BZ), which in $d = 1$ is defined as the interval $k_x \in (-\pi/a, \pi/a]$. The emergence of a BZ is a result of the periodicity of the Hamiltonian and connects to the Bloch theorem [12]. According to the latter, the eigenvector $\boldsymbol{\phi}(\boldsymbol{r})$ of a periodic Hamiltonian satisfying $\hat{H}(\boldsymbol{r} + na\check{\boldsymbol{x}} + mb\check{\boldsymbol{y}} + lc\check{\boldsymbol{z}}) = \hat{H}(\boldsymbol{r})$, with $n, l, m, \in \mathbb{Z}$, can be decomposed into two parts: $\boldsymbol{\phi}(\boldsymbol{r}) = \sum_{\boldsymbol{k}} \boldsymbol{u}_{\boldsymbol{k}}(\boldsymbol{r}) e^{\mathrm{i}\boldsymbol{k}\cdot\boldsymbol{r}}$. Here $\boldsymbol{u}_{\boldsymbol{k}}(\boldsymbol{r})$ has the same periodicity as the Hamiltonian and $\boldsymbol{k}$ is defined in the 1st BZ. In the case of a crystal, the electrons feel a periodic ionic potential, $V(\boldsymbol{r} + na\check{\boldsymbol{x}} + mb\check{\boldsymbol{y}} + lc\check{\boldsymbol{z}}) = V(\boldsymbol{r})$, and the corresponding eigenvectors $\boldsymbol{u}_{\boldsymbol{k}}(\boldsymbol{r})$ satisfy the time-independent Schrödinger equation

$$\left[\frac{(\hat{\boldsymbol{p}} + \hbar\boldsymbol{k})^2}{2m} + V(\boldsymbol{r})\right]\boldsymbol{u}_{\boldsymbol{k}}(\boldsymbol{r}) = E_{\boldsymbol{k}}\boldsymbol{u}_{\boldsymbol{k}}(\boldsymbol{r}). \tag{1.18}$$

The energy bandstructure $E_{\boldsymbol{k},n}$ of a crystal is determined by retrieving the eigenstates $\boldsymbol{u}_{\boldsymbol{k},n}(\boldsymbol{r})$ of the Bloch Hamiltonian, identified as the operator on the left-hand side (lhs) of the above equation.

Before concluding this paragraph, let us retrieve the transformation properties of the single-particle spinor wavefunction $\boldsymbol{u}_{\boldsymbol{k}}(\boldsymbol{r})$ and the Bloch Hamiltonian under K, which is useful for analysing the topological properties of the crystalline materials to be discussed in the upcoming chapters. The complete electronic wavefunction is $\boldsymbol{\phi}(\boldsymbol{r}) = \sum_{\boldsymbol{k}} \boldsymbol{u}_{\boldsymbol{k}}(\boldsymbol{r}) e^{\mathrm{i}\boldsymbol{k}\cdot\boldsymbol{r}}$ and under the action of K one obtains

$$K\boldsymbol{\phi}(\boldsymbol{r}) = \sum_{\boldsymbol{k}} \boldsymbol{u}_{\boldsymbol{k}}^*(\boldsymbol{r}) e^{-\mathrm{i}\boldsymbol{k}\cdot\boldsymbol{r}} \equiv \sum_{\boldsymbol{k}} \boldsymbol{u}_{-\boldsymbol{k}}^*(\boldsymbol{r}) e^{\mathrm{i}\boldsymbol{k}\cdot\boldsymbol{r}}. \tag{1.19}$$

One observes that the action of K on the complete wavefunction can be completely absorbed in taking the complex conjugate of $\boldsymbol{u}_{\boldsymbol{k}}(\boldsymbol{r})$ and inverting its wavevector index. The latter implies the following action of K on a Bloch Hamiltonian

$$K\hat{H}_{\boldsymbol{k}}(\boldsymbol{r}) = \hat{H}^{*}_{-\boldsymbol{k}}(\boldsymbol{r}). \tag{1.20}$$

Note that the wavevector satisfies $K\boldsymbol{k} = \boldsymbol{k}$. In contrast, $K\hbar\boldsymbol{k} = -\hbar\boldsymbol{k}$, which follows from $K\hat{\boldsymbol{p}} = -\hat{\boldsymbol{p}}$. Due to this difference, equation (1.19) leads to the inversion of the wavevector appearing in the right-hand side (rhs) of equation (1.20), and guarantees the consistency between the $\boldsymbol{r}$- and $\boldsymbol{k}$-space descriptions.

1.2 Effective Hamiltonians for bulk III–V semiconductors

In the following paragraphs we demonstrate how to employ the symmetry artillery developed above, to phenomenologically construct effective Hamiltonians for III–V semiconductors. These materials are particularly interesting, since they can feature strong spin–orbit coupling (SOC) [1, 4], which is a key ingredient for engineering topological systems [13, 14]. Typically, a semiconductor belonging to this family consists of two chemical elements, having 3 and 5 electrons in their outer atomic shell, which mainly consists of s and p atomic orbitals. Characteristic examples are: GaAs, InAs and InP. The electrons in these semiconductors are not free but instead feel a crystalline potential that results in an energy bandstructure, as in equation (1.18). These semiconductors usually crystallise in the so-called zincblende or wurtzite structures, invariant correspondingly under the T_d and C_{6v} point groups, both lacking a center of inversion [15, 16]. As we discuss in section 1.2.3, bulk inversion asymmetry results in a non-negligible SOC, which can play a pivotal role for crafting topologically non-trivial materials.

Despite the complex spaghetti-like energy bandstructure obtained for these systems, most of the time we are interested in the energetically low lying properties and thus restrict ourselves to the vicinity of particular $\boldsymbol{k}$-space points, about which we obtain a Taylor expansion of the energy dispersion. Usually, these $\boldsymbol{k}$-points constitute local bandstructure extrema and are governed by the same or reduced crystalline symmetry of the system, which sets constraints to the allowed terms in this expansion. This perturbative approach is termed '$\boldsymbol{k}\cdot\boldsymbol{p}$ expansion'. Such an effective Hamiltonian for the given $\boldsymbol{k}$-region can be extracted using a first-principles calculation. However, another approach is to solely rely on the symmetry properties of the system and phenomenologically derive an effective low energy Hamiltonian, sufficient for making qualitative predictions. Importantly, the latter approach can be useful for understanding the universal properties emerging in a broader class of systems, all sharing the same symmetry characteristics and being described by the same type of low energy Hamiltonian.

1.2.1 Effective Hamiltonian about the Γ-point: plain vanilla model

In the following paragraphs we construct an effective model for a semiconductor in $d = 3$, valid near the vicinity of the Γ-point ($\boldsymbol{k} = \boldsymbol{0}$) of the bandstructure. The semiconductor is here assumed to be invariant under inversion and arbitrary rotations. The discussion of crystalline effects, and also bulk and structural inversion asymmetry, is postponed for sections 1.2.2, 1.2.3 and 1.2.4. Our model Hamiltonian builds upon s and p atomic orbitals characterised by the $\ell = 0$ and $\ell = 1$ quantum numbers of the orbital angular momentum. However, the electron spin is characterised by a spin quantum number $s = 1/2$. If we further consider the case of a non-negligible SOC, the orbital and spin angular momenta couple. Under the artificially-enhanced

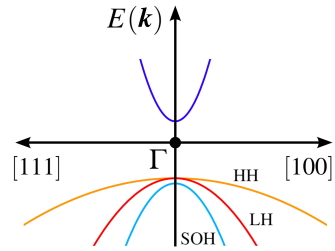

Figure 1.2. Typical bandstructure for a III–V cubic semiconductor near the Γ-point, located at $\boldsymbol{k} = (0, 0, 0)$, that enjoys the full symmetry of the respective point group. The *s* orbitals give rise to the conduction band that appears for positive energies. In contrast, the *p* orbitals yield the three valence hole bands. The latter consist of the heavy (HH), light (LH) and split-off (SOH) hole bands. The HH and LH belong to the same irreducible representation of the point group, which implies their degeneracy at the Γ-point. In addition, all the bands are two-fold degenerate by virtue of time-reversal symmetry. Note, that, there exist materials in this family which exhibit an inverted bandstructure, i.e. the conduction and the top-hole (HH and LH) bands exchange positions, see figure 7.1. As we discuss in chapter 7, the phenomenon of band inversion plays an important role in obtaining topologically-non-trivial semiconductors.

symmetry considered here, it is convenient to introduce the total angular momentum, $\hat{\boldsymbol{J}} = \hat{\boldsymbol{L}} + \hat{\boldsymbol{S}}$. By employing the total angular momentum, we can label the states using the corresponding quantum number j. For the *s* orbitals we obtain $j = 1/2$ and for the *p* orbitals $j = 3/2, 1/2$. The former and latter yield correspondingly the so-called conduction and valence bands. One observes that the valence band consists of two different kinds of states. The $j = 3/2$ leads to the heavy (HH) and light (LH) holes, while the remaining $j = 1/2$ corresponds to the so-called split-off hole (SOH) band, as shown in figure 1.2. Since the HH and LH belong to a different irreducible representation compared to the SOH, the energy values of the bandstructure at the Γ-point of the former and the latter will generally differ unless an accidental degeneracy occurs. Below, we obtain effective Hamiltonians describing the conduction, HH and LH, and SOH bands, in the case where the respective energy splittings at the Γ-point are sufficiently large. Otherwise all these bands are described by an 8×8 Kane model, see [15].

Conduction and split-off hole bands

The effective Hamiltonian has the same general form for these bands, since they are dictated by the same total angular momentum quantum number, i.e. $j = 1/2$. By virtue of inversion symmetry, the terms appearing in the effective Hamiltonian of the conduction and SOH bands have to be even in $\boldsymbol{k}$. In addition, TRS implies that for every Hamiltonian term we should have the same order of powers in $\boldsymbol{k}$ and $\hat{\boldsymbol{J}}$. By additionally taking into account that both $\boldsymbol{k}$ and $\hat{\boldsymbol{J}}$ transform as vectors under rotations, the only couplings allowed have the form $(\boldsymbol{k} \cdot \hat{\boldsymbol{J}})^{2n}$ with $n \in \mathbb{N}$. However, for $j = 1/2$ we obtain $(\boldsymbol{k} \cdot \hat{\boldsymbol{J}})^{2n} \equiv (\hbar^2 \boldsymbol{k}^2/4)^n$, since $\hat{\boldsymbol{J}} = \hbar\hat{\boldsymbol{\tau}}/2$. Here $\hat{\boldsymbol{\tau}}$ correspond to Pauli matrices satisfying $(\boldsymbol{a} \cdot \hat{\boldsymbol{\tau}})^2 = \boldsymbol{a}^2$. Thus, we conclude that the effective Hamiltonians for the conduction and SOH bands, at lowest order in $\boldsymbol{k}$, take the simple form of a quadratic energy dispersion, i.e. $\sim \boldsymbol{k}^2$, as in figure 1.2.

Heavy- and light-hole bands: Luttinger Hamiltonian

Similar symmetry arguments hold for the HH and LH bands, and the allowed Hamiltonian terms have once again the form $(\boldsymbol{k}\cdot\hat{\boldsymbol{J}})^{2n}$ with $n\in\mathbb{N}$. However, for $j=3/2$, the representation of $\hat{\boldsymbol{J}}$ is such that the simplifications encountered in the previous paragraph are not met here. Thus, one retrieves the so-called Luttinger Hamiltonian [17] for a paramagnetic semiconductor, a specific form of which reads

$$\hat{H}(\boldsymbol{k})=\frac{1}{2m}\left[\left(\gamma_1+\frac{5}{2}\gamma_2\right)(\hbar\boldsymbol{k})^2-2\gamma_2(\boldsymbol{k}\cdot\hat{\boldsymbol{J}})^2\right]. \tag{1.21}$$

In more detail, the total angular momentum components can be calculated using the formulas [1]:

$$\begin{aligned}&\hat{J}_{\pm}|j,\,m_j\rangle=\hbar\sqrt{j(j+1)-m_j(m_j\pm1)}\,|j,\,m_j\pm1\rangle\quad\text{and}\\&\hat{J}_z|j,\,m_j\rangle=\hbar m_j|j,\,m_j\rangle,\end{aligned} \tag{1.22}$$

with $\hat{J}_{\pm}=\hat{J}_x\pm\mathrm{i}\hat{J}_y$. By considering the basis $\{|3/2,\,3/2\rangle,\,|3/2,\,1/2\rangle,\,|3/2,\,-1/2\rangle,\,|3/2,\,-3/2\rangle\}$, the above lead to the matrix representations

$$\hat{J}_x=\hbar\begin{pmatrix}0&\frac{\sqrt{3}}{2}&0&0\\[2pt]\frac{\sqrt{3}}{2}&0&1&0\\[2pt]0&1&0&\frac{\sqrt{3}}{2}\\[2pt]0&0&\frac{\sqrt{3}}{2}&0\end{pmatrix},\quad \hat{J}_y=\hbar\begin{pmatrix}0&-\frac{\sqrt{3}}{2}\mathrm{i}&0&0\\[2pt]+\frac{\sqrt{3}}{2}\mathrm{i}&0&-\mathrm{i}&0\\[2pt]0&+\mathrm{i}&0&-\frac{\sqrt{3}}{2}\mathrm{i}\\[2pt]0&0&+\frac{\sqrt{3}}{2}\mathrm{i}&0\end{pmatrix}\quad\text{and} \tag{1.23}$$

$$\hat{J}_z=\hbar\begin{pmatrix}+\frac{3}{2}&0&0&0\\[2pt]0&+\frac{1}{2}&0&0\\[2pt]0&0&-\frac{1}{2}&0\\[2pt]0&0&0&-\frac{3}{2}\end{pmatrix}. \tag{1.24}$$

By employing Kronecker products of the Pauli matrices, $\hat{\boldsymbol{\tau}}$ and $\hat{\boldsymbol{\sigma}}$, accompanied by the corresponding unit matrices, $\hat{1}_\tau$ and $\hat{1}_\sigma$, we may rewrite the above total angular momentum operators as follows

$$\begin{aligned}&\hat{J}_x/\hbar=\frac{\sqrt{3}}{2}\hat{\sigma}_x+\frac{1}{2}\left(\hat{\tau}_x\hat{\sigma}_x+\hat{\tau}_y\hat{\sigma}_y\right),\quad \hat{J}_y/\hbar=\frac{\sqrt{3}}{2}\hat{\sigma}_y+\frac{1}{2}\left(\hat{\tau}_y\hat{\sigma}_x-\hat{\tau}_x\hat{\sigma}_y\right)\quad\text{and}\\&\hat{J}_z/\hbar=\frac{1}{2}\hat{\sigma}_z+\hat{\tau}_z.\end{aligned} \tag{1.25}$$

Note that throughout this book we adopt this simplified notation, where Kronecker products and unit matrices are omitted, e.g. $\frac{1}{2}\hat{1}_\tau \otimes \hat{\sigma}_z + \hat{\tau}_z \otimes \hat{1}_\sigma \mapsto \frac{1}{2}\hat{\sigma}_z + \hat{\tau}_z$.

Since the Luttinger Hamiltonian is made of products of the different components of the total angular momentum, i.e. $\hat{J}_a\hat{J}_b$ with $a, b = x, y, z$, it is convenient to introduce the $\hat{\Gamma}_{1,2,3,4,5}$ matrices, as employed in reference [18]

$$\hat{\Gamma}_1 = \hat{\tau}_z\hat{\sigma}_x, \quad \hat{\Gamma}_2 = \hat{\tau}_z\hat{\sigma}_y, \quad \hat{\Gamma}_3 = \hat{\tau}_z\hat{\sigma}_z, \quad \hat{\Gamma}_4 = \hat{\tau}_x \quad \text{and} \quad \hat{\Gamma}_5 = \hat{\tau}_y. \tag{1.26}$$

The $\hat{\Gamma}$ matrices can be viewed as a vector $\hat{\boldsymbol{\Gamma}}$ in a $d = 5$ space, and constitute the natural extension of the Pauli matrices $\hat{\boldsymbol{\sigma}}$, as they satisfy $\{\hat{\Gamma}_\alpha, \hat{\Gamma}_\beta\} = 2\delta_{\alpha,\beta}\hat{1}_\Gamma$. Furthermore, they also connect to the $\hat{\gamma}$ matrices appearing in the Dirac equation. With the use of $\hat{\boldsymbol{\Gamma}}$, the Hamiltonian is compactly written as

$$\hat{H}(\boldsymbol{k}) = \varepsilon(\boldsymbol{k})\hat{1}_\Gamma - V\boldsymbol{g}(\boldsymbol{k}) \cdot \hat{\boldsymbol{\Gamma}}, \tag{1.27}$$

with $\varepsilon(\boldsymbol{k}) = \frac{\gamma_1}{2m}(\hbar\boldsymbol{k})^2$ and $V = \frac{\gamma_2}{2m}\sqrt{3}\,\hbar^2$, while the vector $\boldsymbol{g}(\boldsymbol{k})$ is defined as

$$g_1(\boldsymbol{k}) = 2k_xk_z, \quad g_2(\boldsymbol{k}) = 2k_yk_z, \quad g_3(\boldsymbol{k}) = \frac{2k_z^2 - k_x^2 - k_y^2}{\sqrt{3}}, \tag{1.28}$$

$$g_4(\boldsymbol{k}) = k_x^2 - k_y^2 \quad \text{and} \quad g_5(\boldsymbol{k}) = 2k_xk_y. \tag{1.29}$$

Interestingly, the $g_\alpha(\boldsymbol{k})$ correspond to the $\ell = 2$ spherical harmonics that transform according to the respective irreducible representation of SO(3). The eigenenergies of the above Hamiltonian read

$$E_\pm(\boldsymbol{k}) = \varepsilon(\boldsymbol{k}) \pm V|\boldsymbol{g}(\boldsymbol{k})| = \frac{\gamma_1 \pm 2\gamma_2}{2m}(\hbar\boldsymbol{k})^2, \tag{1.30}$$

and exhibit a Kramers degeneracy due to TRS. The labels + and − correspond to the LH and HH bands, and one observes that the energy dispersions reflect the bandstructure depicted in figure 1.2.

1.2.2 Cubic crystalline effects and double covering groups

While in the above we neglected the crystalline effects for simplicity, in this paragraph we restore them and understand their impact on the form of the effective Hamiltonian derived. Here we continue to keep the inversion-symmetry intact and discuss the consequences of its violation in the upcoming subsections. The relevant cubic point group preserving I is the O_h, which consists of 48 elements as shown by its character table presented in table 1.3.

One finds that the wavevector $\boldsymbol{k}$ transforms according to the T_{1u} irreducible representation, while the total angular momentum $\hat{\boldsymbol{J}}$ belongs to the T_{1g}. Note that the index g/u (gerade/ungerade) reflects that the respective quantity is even/odd under I. Due to this difference, no linear terms in $\boldsymbol{k}$ are allowed. Specifically, the product of two operators transforming according to the T_{1u} and T_{1g} irreducible representations yield operators that transform according to one of the following: A_{1u}, E_u, T_{1u}

Table 1.3. Character table of the O_h point group. See reference [2].

O_h	E	$8C_3$	$6C_2$	$6C_4$	$3C_2$	I	$6S_4$	$8S_6$	$3\sigma_h$	$6\sigma_d$
A_{1g}	1	1	1	1	1	1	1	1	1	1
A_{2g}	1	1	−1	−1	1	1	−1	1	1	−1
E_g	2	−1	0	0	2	2	0	−1	2	0
T_{1g}	3	0	−1	1	−1	3	1	0	−1	−1
T_{2g}	3	0	1	−1	−1	3	−1	0	−1	1
A_{1u}	1	1	1	1	1	−1	−1	−1	−1	−1
A_{2u}	1	1	−1	−1	1	−1	1	−1	−1	1
E_u	2	−1	0	0	2	−2	0	1	−2	0
T_{1u}	3	0	−1	1	−1	−3	−1	0	1	1
T_{2u}	3	0	1	−1	−1	−3	1	0	1	−1

and T_{2u} irreducible representations. The latter is expressed as $T_{1u} \times T_{1g} = A_{1u} + E_u + T_{1u} + T_{2u}$. Thus, only one combination of these three-dimensional irreducible representations can lead to a scalar or equivalently a one-dimensional irreducible representation. This occurs via the inner product $\boldsymbol{k} \cdot \hat{\boldsymbol{J}}$, that belongs to the A_{1u}. However, only terms transforming according to the identity irreducible representation (A_{1g}) can appear in the Hamiltonian. We observe that $A_{1u} \times A_{1u} = A_{1g}$ and consequently even powers of $\boldsymbol{k} \cdot \hat{\boldsymbol{J}}$ are legitimate candidates. This is in agreement with the Luttinger Hamiltonian retrieved earlier and arises due to the fact that the O_h point group supports three-dimensional irreducible representations, similar to the continuous rotational groups.

At this point a remark is in place. In section 1.1 we argued that the rotation operator for a half-integer spin is 4π-periodic with respect to the rotation angle. From a mathematical point of view, this stems from the fact that the elements of spin rotations in this case belong to the so-called SU(2) group, being the double covering of the SO(3) group of rotations in Euclidean $d = 3$ space [1]. As we remarked in section 1.1, the wavefuctions can be labelled by the irreducible representations of the total angular momentum, while the observables by the irreducible representations of the orbital angular momentum. In other words, the spinors transform according to the SU(2) group and the observables according to the SO(3) group. In a similar fashion, when crystalline symmetry is introduced, the observables transform according to the irreducible representations of the point group and the spinors according to the ones of the double covering point group. To retrieve the irreducible representations of the latter, one has to extend the domain of the rotation angles from $[0, 2\pi)$ to $[0, 4\pi)$. This becomes possible by introducing an additional point-group element E', that corresponds to a rotation of 2π and therefore satisfies $(E')^2 = E$. In this manner, if the ensuing point group consists of $h_{\mathcal{G}}$ elements labelled by g_i, the introduction of E' will double them, since the elements $E'g_i$ will be added. Thereafter, the procedure for determining the new irreducible representations and character table follows section 1.1.4. In the Hands-on section 1.3 we give instructions for obtaining the double covering group of C_{3v}.

Table 1.4. Character table of the T_d point group. See reference [2].

T_d	E	$8C_3$	$3C_2$	$6S_4$	$6\sigma_d$	Linear	Higher order
A_1	1	1	1	1	1	–	$k_x^2 + k_y^2 + k_z^2$, $k_x k_y k_z$
A_2	1	1	1	−1	−1	–	–
E	2	−1	2	0	0	–	$\left(2k_z^2 - k_x^2 - k_y^2, k_x^2 - k_y^2\right)$
T_1	3	0	−1	1	−1	$\hat{\boldsymbol{J}}$	$\left(k_x\left(k_y^2 - k_z^2\right), k_y\left(k_z^2 - k_x^2\right), k_z\left(k_x^2 - k_y^2\right)\right)$
T_2	3	0	−1	−1	1	$\boldsymbol{k}$	$(k_x k_y, k_x k_z, k_y k_z)$

1.2.3 Bulk inversion asymmetry

In the previous paragraphs we considered an I-symmetric semiconductor. However, this symmetry is violated in reality. Breaking inversion reduces the point-group symmetry from O_h, to its T_d subgroup, having a character table presented in table 1.4. In the former table we also added examples of linear, quadratic and cubic terms transforming according to the irreducible representations of T_d. We immediately observe that even when inversion is broken, no bilinear coupling of the form $\boldsymbol{k} \cdot \hat{\boldsymbol{J}}$ is allowed, since $T_1 \times T_2 = A_2 + E + T_1 + T_2$ does not include A_1. However, a coupling cubic in $\boldsymbol{k}$ and linear in $\hat{\boldsymbol{J}}$ is now permitted. The latter is the so-called Dresselhaus SOC [15] and has the following form

$$\hat{H}_D(\boldsymbol{k}) = \lambda\left[\left(k_y^2 - k_z^2\right)k_x\hat{J}_x + \left(k_z^2 - k_x^2\right)k_y\hat{J}_y + \left(k_x^2 - k_y^2\right)k_z\hat{J}_z\right], \tag{1.31}$$

with λ denoting a variable parametrising its strength. Due to the linear coupling to the total angular momentum, such a Hamiltonian can be equivalently viewed as a $\boldsymbol{k}$-dependent magnetic field. Note that such a term appears for both the conduction and valence bands, while it constitutes the lowest order SOC term in $\boldsymbol{k}$, appearing for the conduction band. Finally, we have to remark that a coupling linear in $\boldsymbol{k}$ and cubic in $\hat{\boldsymbol{J}}$ is also possible for the HH and LH bands.

1.2.4 Confinement and structural inversion asymmetry

Apart from bulk semiconductors, confined systems such as quantum wells, nanowires and dots are also of exceptionally high importance and relevance for designing topological systems [13, 14]. A confinement potential $V_{\text{conf}}(\boldsymbol{r})$ leads to an electric field $\boldsymbol{E}_{\text{conf}}(\boldsymbol{r}) = -\nabla V_{\text{conf}}(\boldsymbol{r})$ that violates inversion and translational symmetries. If we assume for simplicity that $V_{\text{conf}}(\boldsymbol{r}) = V_{\text{conf}}(z)$ implying $\boldsymbol{E}_{\text{conf}}(\boldsymbol{r}) = E(z)\check{\boldsymbol{z}}$, then translational invariance is only broken along the $\check{\boldsymbol{z}}$ direction and solely the k_z wavevector does not constitute a good quantum number any more. In contrast, the perpendicular wavevector $\boldsymbol{k}_\perp = (k_x, k_y)$ and energy are conserved. In this case energy level quantisation takes place, and the k_z quantum number is replaced by a new quantum number associated with confinement.

As an example, let us consider a three-dimensional electron gas with kinetic energy $\hat{\boldsymbol{p}}^2/(2m)$ in the presence of a confinement potential $V_{\text{conf}}(z) = 0\ \forall\, z \in [0, L_z]$ and $V_{\text{conf}}(z) = +\infty\ \forall\, z \in (-\infty, 0) \cup (L_z, +\infty)$. The problem is identical to a particle

in a box with the difference that the particle can still move freely in the xy plane. The eigenstates and eigenergies of the resulting quantum well read

$$\phi_{\boldsymbol{k}_\perp,n}(\boldsymbol{r}) = \sqrt{\frac{2}{L_z}} \sin\left(\frac{n\pi z}{L_z}\right) e^{i(k_x x + k_y y)} \quad \text{and} \quad E_n(\boldsymbol{k}_\perp) = \frac{\hbar^2 (n\pi)^2}{2mL_z^2} + \frac{(\hbar \boldsymbol{k}_\perp)^2}{2m}, \tag{1.32}$$

with $n = 1, 2, \ldots, +\infty$. A quantum nanowire (dot) is obtained when further confining one (two) extra dimension(s).

While the above appears to be the whole story, this is fortunately not true. More interesting phenomena occur due to confinement and the resulting *structural inversion asymmetry*. The latter can be taken into account by recalling that the non-relativistic Schrödinger equation is obtained as a limit of Dirac's equation. As a result of this limiting procedure an additional term appears which is proportional to $(\hat{\boldsymbol{p}} \times \hat{\boldsymbol{\sigma}}) \cdot \boldsymbol{E}$ [1], with $\hat{\boldsymbol{\sigma}}$ denoting the spin Pauli matrices. When inversion symmetry is present, $\boldsymbol{E} = \boldsymbol{0}$, and thus this term drops out. For the quantum well case, this term is present and leads to the so-called Rashba SOC given by the Hamiltonian

$$\hat{H}_R(\boldsymbol{k}) = \alpha\hbar\left(k_x\hat{\sigma}_y - k_y\hat{\sigma}_x\right). \tag{1.33}$$

Similar effects arise in crystalline systems, the only difference being that the ionic potential generally yields more complicated SOC terms. In the following paragraphs we focus, for simplicity, on the conduction band near the Γ-point of a III–V semiconductor with bulk inversion asymmetry for different directions of the confinement-imposed electric field.

Confinement within the (001) plane: C_{2v} point-group symmetry

In this paragraph we consider the Γ-point conduction band of a zincblende III–V semiconductor with T_d point-group symmetry, whose Hamiltonian reads

$$\hat{H}_c(\boldsymbol{k}) = \frac{(\hbar \boldsymbol{k})^2}{2m} + E_c + \lambda\left[\left(k_y^2 - k_z^2\right)k_x\hat{\tau}_x + \left(k_z^2 - k_x^2\right)k_y\hat{\tau}_y + \left(k_x^2 - k_y^2\right)k_z\hat{\tau}_z\right]. \tag{1.34}$$

The $\hat{\boldsymbol{\tau}}$ Pauli matrices above act on the total angular momentum Kramers doublet, which corresponds to the Γ_6 irreducible representation of the double covering T_d group[1] [15]. We further assume that the system is confined, by applying an electric field along the $\check{\boldsymbol{z}}$ direction. Using Miller indices[2] [12], the xy confinement plane is denoted by (001). According to [19], the confinement reduces the point-group symmetry of the system to C_{2v}, and invalidates k_z as a good quantum number. As a

[1] In contrast, the SOH (HH and LH) band(s) transform according to the Γ_7 (Γ_8) irreducible representation of the double covering T_d point group.

[2] The Miller indices (hkl), define a plane in reciprocal space which is normal to the reciprocal ($\boldsymbol{k}$) space vector $h\boldsymbol{b}_1 + k\boldsymbol{b}_2 + l\boldsymbol{b}_3$, with $\boldsymbol{b}_{1,2,3}$ denoting the reciprocal lattice basis vectors. Note that for a cubic system, the reciprocal lattice vectors coincide with the direct ($\boldsymbol{r}$-space) lattice basis vectors, generally denoted with $\boldsymbol{a}_{1,2,3}$. With the Miller indices [hkl], we denote the direction $h\boldsymbol{a}_1 + k\boldsymbol{a}_2 + l\boldsymbol{a}_3$, in the direct lattice.

result of confinement, the Hamiltonian above becomes a matrix in the confinement eigenstate basis, with matrix elements

$$\begin{aligned}\hat{H}_{c,nm}(\boldsymbol{k}_\perp) &= \left[\frac{(\hbar \boldsymbol{k}_\perp)^2}{2m} + E_{c,n}\right]\delta_{n,m} \\ &+ \lambda\left\{\left[k_y^2\delta_{n,m} - \left\langle k_z^2\right\rangle_{nm}\right]k_x\hat{\tau}_x + \left[\left\langle k_z^2\right\rangle_{nm} - k_x^2\delta_{n,m}\right]k_y\hat{\tau}_y + \left(k_x^2 - k_y^2\right)\langle k_z\rangle_{nm}\hat{\tau}_z\right\}.\end{aligned} \tag{1.35}$$

The matrix elements $\langle k_z\rangle_{nm}$ and $\langle k_z^2\rangle_{nm}$ are understood as appropriate matrix elements in the confinement eigenstate basis that replace k_z and k_z^2, respectively. In the extreme limit that crystalline effects along the z axis become negligible, the former are matrix elements of the rescaled momentum operator $\hat{p}_z/\hbar$. Since here we attempt to acquire a phenomenological understanding, it only suffices that these matrix elements are non zero. When confinement is strong, we may restrict to the energetically lowest confinement eigenstate, as given by the $E_{c,n}$ hierarchy. In the single channel approximation, we obtain $\langle k_z\rangle_{nm} \mapsto \langle k_z\rangle$ and $\langle k_z^2\rangle_{nm} \mapsto \langle k_z^2\rangle$ and we may drop the n, m indices in the Hamiltonian of equation (1.35). For a single channel $\langle k_z\rangle = 0$, since the confinement channel wavefunction is real. Thus, by restricting to up to the quadratic order in the wavevector, we obtain the effective Hamiltonian

$$\hat{H}_{c,\text{lowest}}(\boldsymbol{k}_\perp) = \frac{(\hbar \boldsymbol{k}_\perp)^2}{2m} + E_{c,\text{lowest}} - \lambda\langle k_z^2\rangle\left(k_x\hat{\tau}_x - k_y\hat{\tau}_y\right). \tag{1.36}$$

Note that this result contains only the projected bulk Hamiltonian and the Dresselhaus effect. The effects of structural inversion asymmetry have not been included yet and after adding them we obtain the final effective (001) Hamiltonian up to the quadratic order

$$\hat{H}^{(001)}_{c,\text{lowest}}(\boldsymbol{k}_\perp) = \frac{(\hbar \boldsymbol{k}_\perp)^2}{2m} + E_{c,\text{lowest}} - \lambda\langle k_z^2\rangle\left(k_x\hat{\tau}_x - k_y\hat{\tau}_y\right) + \left(|\alpha_{xy}|k_x\hat{\tau}_y - |\alpha_{yx}|k_y\hat{\tau}_x\right). \tag{1.37}$$

Note that the C_{2v} point group allows for an anisotropic Rashba SOC term.

Finally, note that in the case of an inversion-symmetric bulk semiconductor, $\lambda = 0$, and in the presence of the confinement potential, the point-group symmetry would be reduced to C_{4v}, which would only lead to a Rashba term with $|\alpha_{xy}| = |\alpha_{yx}| \equiv \alpha$.

Confinement within the (111) plane: C_{3v} point-group symmetry

If the bulk semiconductor could be cut or confined in the (111) plane, a C_{3v} point-group symmetry emerges [19], whose properties were studied in section 1.1.4. In table 1.5 we present a list of quantities that transform according to the irreducible representations of this symmetry group.

As in the previous paragraph, one can appropriately project the Hamiltonian of equation (1.34) in order to obtain the Dresselhaus SOC for the quantum well. However, here we employ the predictive power given by knowing the ensuing point-group symmetry, in combination with TRS, so to arrive at the effective Hamiltonian which incorporates both structural and bulk inversion asymmetry types of SOC.

Table 1.5. Quantities transforming according to the irreducible representations of C_{3v}.

Irr. Rep.	E	$2C_3$	$3\sigma_v$	Linear	Higher order
A_1	1	1	1	–	$k_x^2 + k_y^2$, $k_y\left(k_y^2 - 3k_x^2\right)$
A_2	1	1	−1	$\hat{J}_z$	$k_x\left(k_x^2 - 3k_y^2\right)$
E	2	−1	0	(k_x, k_y), $(\hat{J}_y, -\hat{J}_x)$	$\left(2k_xk_y, k_x^2 - k_y^2\right)$, (k_xk_z, k_yk_z)

Since there exist only linear terms in $\hat{\boldsymbol{J}} = \hbar\hat{\boldsymbol{\tau}}/2$ for the given spinor representation, we find the following Hamiltonian

$$\hat{H}^{(111)}_{c,\text{lowest}}(\boldsymbol{k}_\perp) = \frac{(\hbar\boldsymbol{k}_\perp)^2}{2m} + E_{c,\text{lowest}} + \alpha\hbar\left(k_x\hat{\tau}_y - k_y\hat{\tau}_x\right) + \gamma k_x\left(k_x^2 - 3k_y^2\right)\hat{\tau}_z. \tag{1.38}$$

As one observes, for the given symmetry group we obtain a Rashba-like term, as also a cubic in $\boldsymbol{k}$ contribution. By projecting the original Dresselhaus Hamiltonian onto the energetically-lowest confinement eigenstate, one finds that it contributes to both terms.

Finally, note that a Hamiltonian identical to the one presented above, appears also for the topologically protected states on the (111) surface of a bulk topological insulator [20, 21], such as Bi_2Te_3 and Bi_2Se_3. Aspects of these so-called warped topological insulators are discussed in section 7.2.3.

1.3 Hands-on: symmetry analysis of a triple quantum dot

The scope of this section is to help the interested reader become more familiar with the symmetry classification and the construction of effective Hamiltonians. We suggest a number of tasks in relation to the triple quantum dot system introduced in section 1.1.4. For comparison, we provide the answers to the posed questions, and guidance for the required intermediate steps.

To carry out the proposed tasks, it is recommended to introduce the following multicomponent wavefunction:

$$\boldsymbol{\Phi}^{\mathrm{T}} = \left(\phi_{1,\uparrow}, \phi_{1,\downarrow}, \phi_{2,\uparrow}, \phi_{2,\downarrow}, \phi_{3,\uparrow}, \phi_{3,\downarrow}\right), \tag{1.39}$$

in order to describe the spinful electrons defined for the three quantum dots labelled by 1, 2, 3. A general 6×6 Hamiltonian acting on this wavefunction is expressed as a Kronecker product $\hat{\lambda}_\alpha \otimes \hat{\sigma}_b$ ($\alpha = 1, \ldots, 8$ and $b = x, y, z$) of the following SU(3) Gell-Mann [22] $\hat{\lambda}$ matrices

$$\begin{gathered}
\hat{\lambda}_1 = \begin{pmatrix} 0&1&0\\ 1&0&0\\ 0&0&0 \end{pmatrix},\ \hat{\lambda}_2 = \begin{pmatrix} 0&-\mathrm{i}&0\\ \mathrm{i}&0&0\\ 0&0&0 \end{pmatrix},\ \hat{\lambda}_3 = \begin{pmatrix} 1&0&0\\ 0&-1&0\\ 0&0&0 \end{pmatrix},\ \hat{\lambda}_4 = \begin{pmatrix} 0&0&1\\ 0&0&0\\ 1&0&0 \end{pmatrix} \\
\hat{\lambda}_5 = \begin{pmatrix} 0&0&-\mathrm{i}\\ 0&0&0\\ \mathrm{i}&0&0 \end{pmatrix},\ \hat{\lambda}_6 = \begin{pmatrix} 0&0&0\\ 0&0&1\\ 0&1&0 \end{pmatrix},\ \hat{\lambda}_7 = \begin{pmatrix} 0&0&0\\ 0&0&-\mathrm{i}\\ 0&\mathrm{i}&0 \end{pmatrix},\ \hat{\lambda}_8 = \frac{1}{\sqrt{3}}\begin{pmatrix} 1&0&0\\ 0&1&0\\ 0&0&-2 \end{pmatrix}
\end{gathered} \tag{1.40}$$

Table 1.6. Classification of $\hat{\boldsymbol{\lambda}}$ and $\hat{\boldsymbol{\sigma}}$ matrices under $C_{3v} \times \mathcal{T}$.

Irr. Rep.	E	$2C_3$	$3\sigma_v$	$\mathcal{T} = +1$	$\mathcal{T} = -1$
A_1	1	1	1	$\hat{\Lambda}_z, \hat{1}_\sigma, \hat{\lambda}_z^+$	–
A_2	1	1	−1	–	$\hat{\sigma}_z, \hat{\lambda}_z^-$
E	2	−1	0	$\left(\hat{\Lambda}_x, \hat{\Lambda}_y\right), \left(\hat{\lambda}_x^+, \hat{\lambda}_y^+\right)$	$(\hat{\sigma}_y, -\hat{\sigma}_x), \left(\hat{\lambda}_y^-, -\hat{\lambda}_x^-\right)$

acting on the 1, 2, 3 quantum-dot index and the usual $\hat{\boldsymbol{\sigma}}$ Pauli matrices acting on the spin index ↑, ↓. We additionally have the respective unit matrices $\hat{1}_\lambda$ and $\hat{1}_\sigma$. For simplicity we omit the Kronecker-product symbol ⊗, and the unit matrices $\hat{1}_\lambda$ and $\hat{1}_\sigma$. By adopting the active view of symmetry transformations for the C_{3v} point group, proceed with carrying out the tasks.

Task 1: Show that the operators generating the C_3 rotation and the σ_{xz} mirror operation read

$$\hat{C}_3 = \begin{pmatrix} 0\,0\,1 \\ 1\,0\,0 \\ 0\,1\,0 \end{pmatrix} e^{-\mathrm{i}\pi\hat{\sigma}_z/3} \quad \text{and} \quad \hat{\sigma}_{xz} = \begin{pmatrix} 1\,0\,0 \\ 0\,0\,1 \\ 0\,1\,0 \end{pmatrix} \mathrm{i}\hat{\sigma}_y. \tag{1.41}$$

Explain the imaginary 'i' appearing in the expression for $\hat{\sigma}_{xz}$, by embedding the system in $d = 3$ and expressing σ_{xz} as a combination of inversion and a proper rotation. See also section 1.1.

Task 2: Show that the $\hat{\lambda}_{1,\ldots,8}$ and $\hat{\sigma}_{x,y,z}$ matrices are classified according to the irreducible representations of the $C_{3v} \times \mathcal{T}$ symmetry group, as presented in table 1.6 where we have introduced

$$\hat{\boldsymbol{\Lambda}} \equiv \left(\hat{\Lambda}_x, \hat{\Lambda}_y, \hat{\Lambda}_z\right) := \left(\frac{\hat{\lambda}_8 + \sqrt{3}\hat{\lambda}_3}{2}, \frac{\sqrt{3}\hat{\lambda}_8 - \hat{\lambda}_3}{2}, \hat{1}_\lambda\right), \tag{1.42}$$

$$\hat{\boldsymbol{\lambda}}^+ \equiv \left(\hat{\lambda}_x^+, \hat{\lambda}_y^+, \hat{\lambda}_z^+\right) := \left(\frac{\hat{\lambda}_1 + \hat{\lambda}_4 - 2\hat{\lambda}_6}{\sqrt{3}}, \hat{\lambda}_1 - \hat{\lambda}_4, \hat{\lambda}_1 + \hat{\lambda}_4 + \hat{\lambda}_6\right), \tag{1.43}$$

$$\hat{\boldsymbol{\lambda}}^- \equiv \left(\hat{\lambda}_x^-, \hat{\lambda}_y^-, \hat{\lambda}_z^-\right) := \left(\frac{\hat{\lambda}_2 - \hat{\lambda}_5 - 2\hat{\lambda}_7}{\sqrt{3}}, \hat{\lambda}_2 + \hat{\lambda}_5, \hat{\lambda}_2 - \hat{\lambda}_5 + \hat{\lambda}_7\right). \tag{1.44}$$

Task 3: Verify that the most general $C_{3v} \times \mathcal{T}$-symmetric single-particle Hamiltonian has the form

$$\hat{H} = \varepsilon - t_{dd}\hat{\lambda}_z^+ + \alpha\hbar\left(\hat{\lambda}_x^-\hat{\sigma}_x + \hat{\lambda}_y^-\hat{\sigma}_y\right) - \beta\hat{\lambda}_z^-\hat{\sigma}_z. \tag{1.45}$$

Notice the analogy to equation (1.38).

Table 1.7. Character table of the double covering C_{3v} point group.

Irr. Rep.	E	$2C_3$	$3\sigma_v$	E'	$2E'C_3$	$3E'\sigma_v$
A_1	1	1	1	1	1	1
A_2	1	1	−1	1	1	−1
E	2	−1	0	2	−1	0
A_1'	1	−1	i	−1	1	−i
A_2'	1	−1	−i	−1	1	i
E′	2	1	0	−2	−1	0

Task 4: Retrieve the character table for the irreducible representations of the double covering C_{3v} point group, shown in table 1.7. To carry out this task, follow sections 1.1.4 and 1.2.2. Note that the addition of the group element E', doubles the number of elements. In fact, in the present case it additionally doubles the number of irreducible representations. The latter doubling is not generic though, see [4].

References

[1] Messiah A 1999 *Quantum Mechanics* Vol 1 and 2 (New York: Dover Publications)
[2] Tinkham M 2003 *Group Theory and Quantum Mechanics* (New York: Dover Publications)
[3] Lax M J 2012 *Symmetry Principles in Solid State and Molecular Physics* (New York: Dover Publications)
[4] Dresselhaus M S, Dresselhaus G and Jorio A 2008 *Group Theory: Application to the Physics of Condensed Matter* (Berlin, Heidelberg: Springer)
[5] Vergados J D 2017 *Group and Representation theory* (Hackensack, NJ: World Scientific)
[6] Altland A and Zirnbauer M R 1997 *Phys. Rev. B* **55** 1142
[7] Kitaev A 2009 *AIP Conf. Proc.* **1134** 22
[8] Ryu S, Schnyder A P, Furusaki A and Ludwig A W W 2010 *New J. Phys.* **12** 065010
[9] Hsieh C-Y, Shim Y-P, Korkusinski M and Hawrylak P 2012 *Rep. Prog. Phys.* **75** 114501
[10] Kotetes P, Jin P-Q, Marthaler M and Schön G 2014 *Phys. Rev. Lett.* **113** 236801
[11] Ashoori R C 1996 *Nature* **379** 413
[12] Grosso G and Parravicini G P 2014 *Solid State Physics* 2nd edn (Amsterdam: Elsevier)
[13] Hasan M Z and Kane C L 2010 *Rev. Mod. Phys.* **82** 3045
[14] Qi X-L and Zhang S-C 2011 *Rev. Mod. Phys.* **83** 1057
[15] Winkler R 2003 *Spin-Orbit Coupling Effects in Two-Dimensional Electron and Hole Systems* (Berlin: Springer)
[16] Gmitra M and Fabian J 2016 *Phys. Rev. B* **94** 165202
[17] Luttinger J M 1956 *Phys. Rev.* **102** 1030
[18] Murakami S, Nagaosa N and Zhang S-C 2004 *Phys. Rev. B* **69** 235206
[19] Yu P Y and Cardona M 2010 *Fundamentals of Semiconductors: Physics and Materials Properties* (Berlin: Springer)
[20] Chen Y L *et al* 2009 *Science* **325** 178
[21] Fu L 2009 *Phys. Rev. Lett.* **103** 266801
[22] Gell-Mann M 1962 *Phys. Rev.* **125** 1067